2018-04-01

Thin Film Carbon Nanofuses for Permanent Data Storage

Kevin Robert Laughlin
Brigham Young University

Thin Film Carbon Nanofuses for Permanent Data Storage

Kevin Robert Laughlin

A thesis submitted to the faculty of
Brigham Young University
in partial fulfillment of the requirements for the degree of

Master of Science

Robert Davis, Chair
Barry Lunt
David Allred

Department of Physics and Astronomy

Brigham Young University

ABSTRACT

Thin Film Carbon Nanofuses for Permanent Data Storage

Kevin Robert Laughlin
Department of Physics and Astronomy, BYU
Master of Science

We have fabricated nanofuses from thin-film, arc-evaporation carbon for use in permanent data storage. Thin film carbon fuses have fewer fabrication barriers and retain the required resistivity and structural stability to work as a data storage medium. Carbon thin films were characterized for their electrical, microstructural, and chemical bonding properties. Annealing the thin-film carbon in an argon environment at 400°C reduced the resistivity from about $4*10^{-2}$ Ω cm as deposited down to about $5*10^{-4}$ Ω cm, allowing a lower blowing voltage. Nanofuses with widths ranging from 200 nm down to 60 nm were fabricated and tested. They blow with voltages between 2 V and 5.5 V, and the nanofuses remain stable in both a "1" and a "0" state under a constantly applied read voltage of 1 volt for over 90 hours, corresponding to a cumulative time of $>10^{12}$ reads.

Keywords: nanofuse, permanent, data storage, fabrication, electron beam lithography, carbon

ACKNOWLEDGMENTS

I would like to thank my graduate advisors for all of their help in learning and understanding the different aspects of pertaining to this research. I would also like to thank my family for their support and patience with me while working on this.

TABLE OF CONTENTS

LIST OF FIGURES

Chapter 1 Introduction

1.1 Introduction

In just over 60 years, from 1951 to 2013, the amount of data that can be stored digitally on a single data storage device has increased from 224 kilobytes to 88 terabytes[1]. Unfortunately, to achieve these high data densities the mean lifetime of the stored data has been sacrificed. As a result, digital data storage devices such as DVDs, hard drives, and flash memory have a mean lifetime of less than 10 years[2-4]. Possible failure mechanisms of these devices could include atomic diffusion, electro-migration, oxidation, and other chemical changes (figure 1). In order to reliably maintain data for more than 10 years, multiple copies are made and the data is periodically migrated[5]. However these solutions are time consuming, involve additional expense, require complex systems for large data volumes, and can still result in data loss[6-9]. Permanent data storage media requires the long term stability of both the "1" and "0" state of the data. For example, a comparison of conventional and permanent data media for optical and solid state are illustrated in figure 1. Writable CD and DVD optical discs contain organic dyes with limited long term stability. The M-Disc, used for permanent data storage, by contrast uses structural changes in an inorganic layer to store the data (figure 1D). This results in data stability of more than 1000 years[7, 10].

1.2 Modern Data Storage

1.2.1 Hard drives

Hard drives use domains of magnetically aligned material to store bits of data. These magnetic regions can be rewritten. A magnetic read head scans over the spinning hard drive disk

where each of the magnetic domains on the disk is a location in memory. The problem with this storage medium is that the magnetic regions can spontaneously flip over time when they are supposed to remain the same.

1.2.2 Optical disks

A laser is used to locally change the optical reflectivity of a material, resulting in written data. Over time the optical reflectivity can revert or change, obscuring the data bits and making them unreadable. The M-disc is an optical disc using unique materials that will hold data for a millennium but has significantly slower read and write speeds than flash memory.

1.2.3 Flash memory

Uses transistors where charge is forced on and off a floating gate to store the data. The gate is surrounded by an insulator, but charge can still leak and tunnel out of it, changing the bit. Flash memory is a random access memory (RAM) and has no moving parts. These two factors allow flash memory to be read significantly faster than spinning disk devices such as hard drives and optical drives.

1.3 Issues with Data Storage

Solid-state flash memory has become widely used for a variety of reasons including its low power requirements, lack of moving parts, and much higher read/write speeds than optical and magnetic discs. Flash based solid state data storage works by storing charge on a floating gate in a transistor. To write a data bit in flash memory, charge is injected onto the floating gate through a thin insulating layer. However, over a period of years a significant amount of the charge that is stored on the floating gate will tunnel out through the insulator resulting in data instability and loss (illustrated in figure 1)[11, 12]. For the development of permanent solid state

data storage there is a need to transition from charge-based and reversible phase-change media, to irreversible structural based storage mechanisms. These mechanisms could include irreversible phase changes, stable chemical bonding changes, or material displacement. Structurally based data storage using microscale metal fuses was prevalent from the 1970s to 1980s. These metal fuses (figure 1) were the basis for Programmable Read Only Memory, or PROM[13]. An intact fuse allows current to flow, while a blown fuse doesn't allow current to flow, corresponding to a data bit of a 1 or a 0 respectively. At the blowing voltage, the metal in the fuse melts and is displaced, opening up an insulating structural gap. Even though metal fuses use

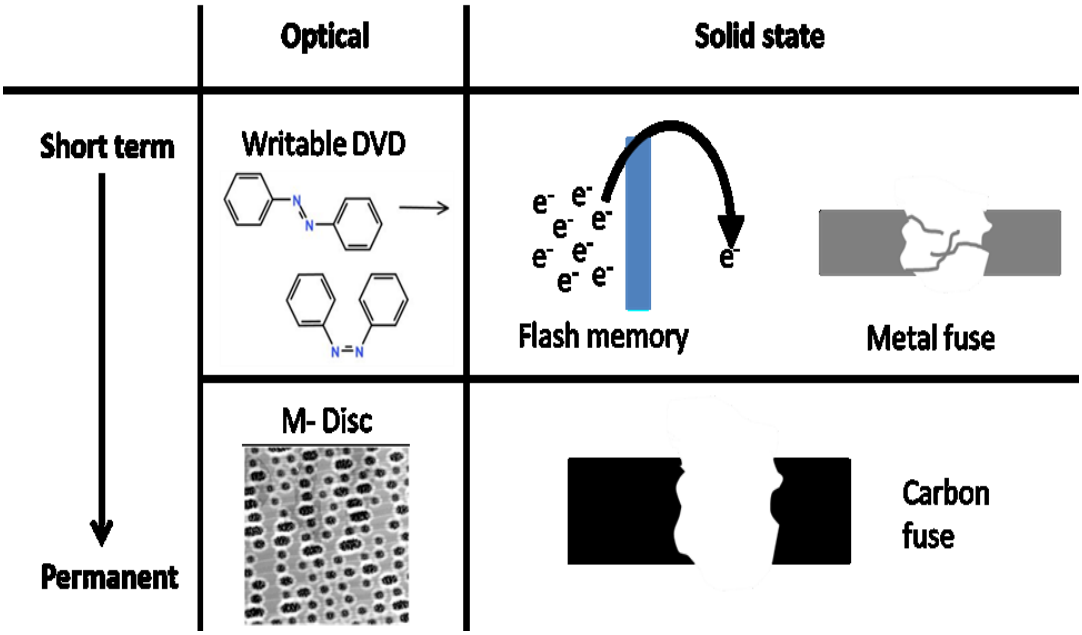

Figure 1 Concept diagram of materials for data storage, from short term to permanent. A) Optical discs can undergo chemical changes resulting in a change of optical properties. B) For IC's tunneling and electro-migration can cause data instability. C) Metal fuses suffer from thermal movement of atoms, resulting in the formation of dendrites. D) The M-Disc is the structurally based permanent data storage device that is currently available. E) Carbon nanofuses use a structural mechanism to store the data, but unlike metal fuses the carbon is stable due to its high local bond strength.

a structural change to store data, the high surface mobility of the metal allows atoms to migrate when a voltage is applied over time[13]. This caused fuses to exhibit dendritic growth in the blown state, forming conductive paths across the fuse gap and resulting in data corruption.

In contrast to metals, conductive graphitic carbon has high structural stability due to its much higher localized bond strength. Graphene is an atomically thin sheet of graphitic carbon, does not readily oxidize below 300 °C, and has thermal and electrical resistivities that could allow fuses to be written in the single volt range. Graphene has recently been used[14] to create carbon fuses where a write voltage permanently oxidized the fuse resulting in a stable structural gap. Consistent with carbon's high local bonding strength, these graphene fuses do not demonstrate dendritic growth. These graphene fuses were fabricated from CVD grown graphene films. CVD graphene layers are polycrystalline, contain grain boundary and other defects and require transfer to an insulating substrate. The grain boundaries, defects, and transfer induced damage of the delicate graphene sheets constitute significant barriers to manufacturing[15, 16]. In short, fabrication of high performance electronic devices with graphene is an active area of research, but there is currently no industrial electronic device manufacturing from graphene due to the significant quality and cost barriers. Conversely, physical vapor deposition of carbon is widely used industrially and consequently can be much more readily integrated into current electronic manufacturing.

Thin-film carbon can be deposited by widely used physical vapor deposition processes, including sputtering, electron beam deposition, and arc-evaporation[17, 18]. Sputtered carbon thin films have resistivities of approximately 10^4 Ω cm[19-21], while arc-evaporation and e-beam evaporated carbon thin films have significantly lower (as deposited) resistivities in the range of 10^{-2} Ω cm[17, 22, 23]. These resistivities can be further lowered by annealing.

Using the relation between temperature, thermal conductivity, and electrical conductivity as described by Pearson[24], a carbon nanofuse will reach the required temperature to be programmed[14] at 3 volts if the resistivity is less than 10^{-2} Ω cm. This means that either arc-evaporation or e-beam evaporated carbon would work for this purpose.

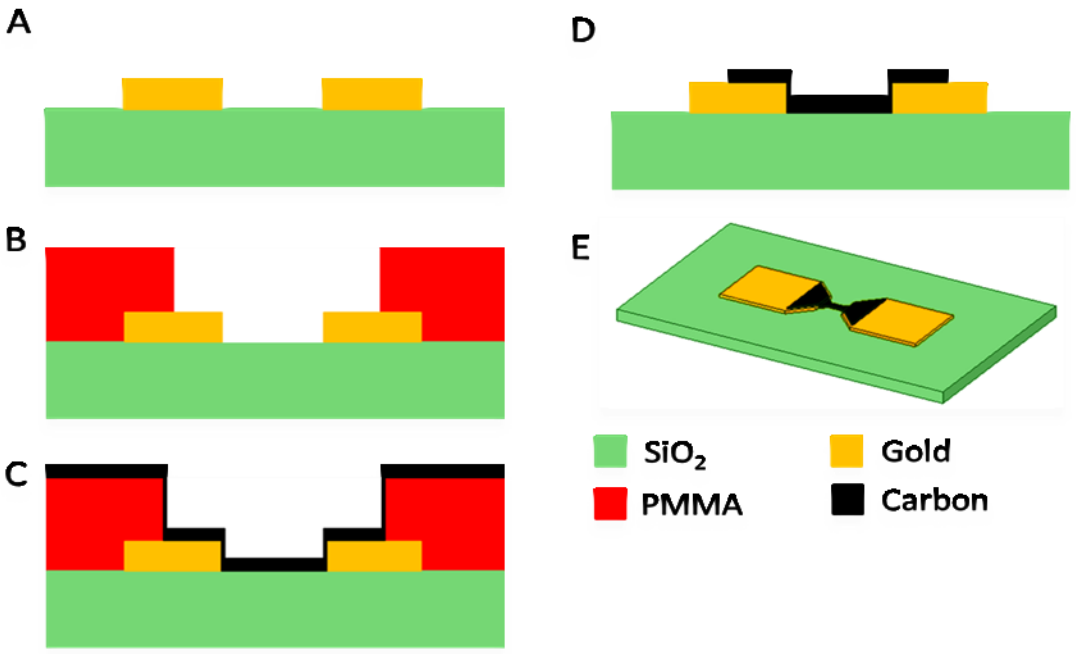

Figure 2 Process flow diagram for fabrication of thin film carbon nanofuses on a silicon dioxide film on a silicon substrate with gold contact pads. A) Gold contact pads with a 5 μm gap are deposited on a silicon dioxide layer. B) PMMA is patterned using electron beam lithography. C) A 20nm thin film carbon layer is deposited using arc-evaporation. D-E) A lift-off process leaves a carbon bow tie pattern electrically connected to the gold contact pads.

We fabricated nanofuses[25] with arc-evaporation carbon, as illustrated in figure 2. When a programming voltage is applied to the fuse, the thin neck of carbon is heated and oxidized. The oxidation process results in a non-conductive gap (a blown fuse). Blown and unblown fuses represent a data bit of a 0 and a 1 respectively. For this study over 100 carbon nanofuses were fabricated and tested with a carbon thickness of 20 nm, a length of 250 nm and widths ranging from 60 nm to 200 nm.

The evaporated carbon represents a significant materials and processing departure from graphene. In contrast to the crystalline monolayer graphene used previously, this evaporated carbon is amorphous and 100 times thicker resulting in significantly different electrical and thermal characteristics. One significant question is whether the time required to blow a fuse with this thicker material will be prohibitive, consequently we made measurements of the data write time and power requirements. The thin-film carbon nanofuses were irreversibly written with low power requirements of between 0.5 and 3.5 milliwatts and with writing speeds less than 200 ns.

Oxidation of a monolayer can happen rapidly but 100 monolayers could act quite differently. This necessitates a measurement of the data write time, which we performed. We also studied the voltage and current requirements for fuses in lateral geometries up to 5 times smaller than the previous work on graphene nanofuses. These studies provide data that will be valuable in determining the feasibility of manufacturing permanent memory from evaporated amorphous carbon and in determining productive fuse geometries.

Decreasing the width of a carbon nanofuse also decreases the voltage and power required to blow them. This allows fuses to be made that will blow at less than 3 volts, which is similar to current Flash memory. Also, when a thin-film carbon nanofuse is blown, dendritic growth has not been observed. No degradation was seen in either the blown or unblown states when held at voltage for a time equivalent to 10^{12} reads.

Chapter 2 Fabrication

Fabrication techniques required to make the carbon nanofuses are: electron beam lithography and physical vapor deposition. Locations and SOPs for the equipment used are in the appendix.

2.1 Electron Beam Lithography

In research facilities, it is common to use Electron Beam Lithography (EBL) to reach feature sizes below 1 μm. For EBL, an electron sensitive chemical (electron resist) is spun onto a flat substrate. Electrons are accelerated to high energies, focused and controlled by magnets down to a few nanometers, and then exposed to the resist in the desired pattern (figure 3B). A chemical change occurs wherever the electrons interact with the resist, either hardening (negative resist) or softening (positive resist) those areas. The resist is then developed, removing the areas of the resist that are more soluble and leaving the desired pattern on the wafer.

For EBL, there are no hard masks. Instead, the desired pattern is first created in a computer-aided design software program which then tells the computer where to send the e-beam. The e-beam is controlled by using magnets to expose the resist with the pattern. Electron beam lithography can achieve feature sizes of a few nanometers, but the downside is that every point in the pattern needs to be exposed. This process can take hours or days for a small area of $1cm^2$ to be exposed. These characteristics make electron beam lithography great for prototyping but not for mass production.

With electron beam lithography, there is a range of doses that resist can be exposed to after it is fully exposed and before it is overexposed. If the pattern is overexposed, the area surrounding the features will become exposed as well resulting in a rounded and larger pattern. If the pattern is underexposed, the exposed resist won't completely develop and the pattern will not transfer. To determine the correct dosage for the electron beam, the desired pattern was exposed multiple times with doses ranging from too low (1 $\mu C/cm^2$) to too high (1000 $\mu C/cm^2$). The exposure that was closest to the desired pattern was identified, and then the process was

repeated, narrowing down the window of exposures. This happened until the correct exposure was found for a given pattern.

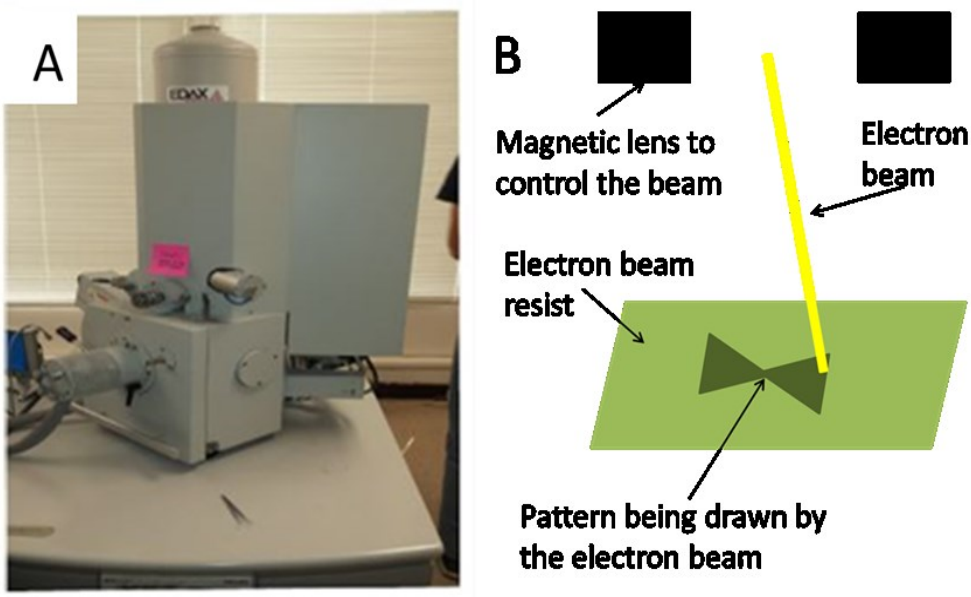

Figure 3 Electron beam lithography A) Image of the SFEG XL30 ESEM used for electron beam lithography. B) Schematic of electron beam lithography. The electron beam is controlled by magnetic lenses, exposing a desired pattern to the electron beam resist.

Electron beam lithography was done with the FEI XL30 ESEM (figure 3A) at BYU equipped with a high speed beam blanker and the Nanometer Patterning Generation System from J.C. Nabity (Bozeman, Montana). These hardware and software additions temporarily convert a scanning electron microscope into an electron beam lithography system.

2.2 Deposition methods

Chrome, gold, and carbon were deposited using thermal and arc-evaporation techniques. These processes vaporize a material to uniformly deposit it onto a flat surface (figure 4). To deposit materials using these methods, the sample is placed in a vacuum tight chamber and pumped down to a pressure of $5*10^{-6}$ Torr.

To deposit gold (figure 4A), current is passed through an alumina coated tungsten coil until the gold melts and then evaporates. The evaporated gold then travels in a line of sight trajectory and solidifies wherever it hits. Because gold does not adhere to SiO_2, a thin layer of chrome is needed as an adhesion layer. Gold then needs to be deposited onto the chrome without breaking vacuum. To deposit chrome (figure 4A), a chrome coated tungsten rod is heated by passing a current through it, until the chrome sublimes.

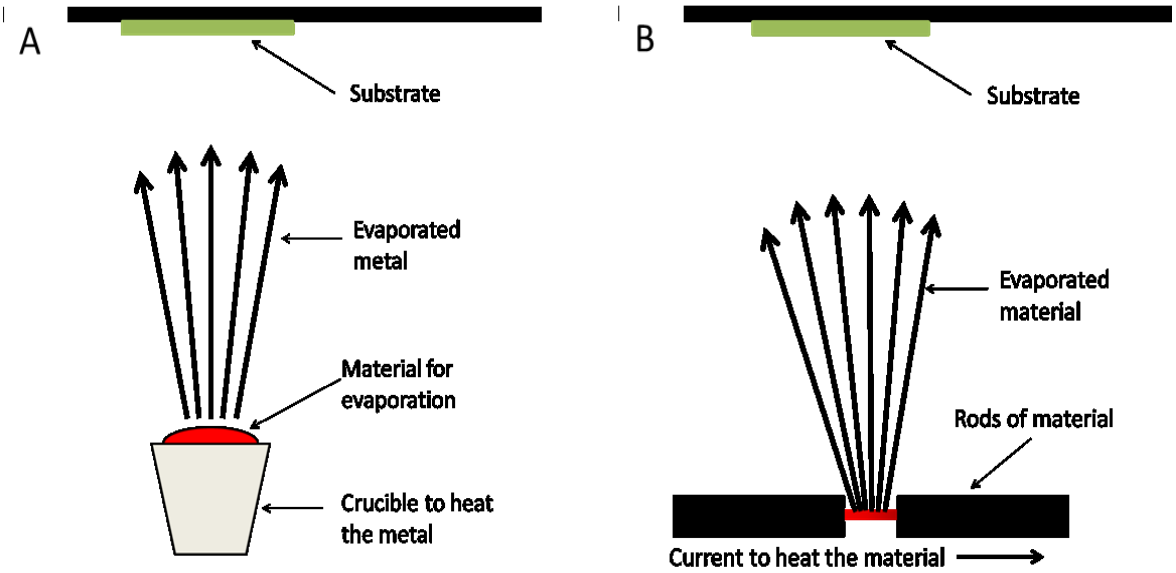

Figure 4 Deposition techniques for gold, chrome, and carbon. A) Gold is heated in a crucible until it evaporates and leaves the crucible in a line of sight path. B) A large current is passed through rods consisting of either chrome or carbon, until the material is heated sufficiently to sublime.

To deposit carbon, a carbon rod was sharpened to a cylindrical point, with a length of 5.5 mm, and an inner width of 1.25 mm and brought together with the flat side of another rod (figure 4B). A high current is passed through the rods, heating up the sharpened area more than the rest of the rods. The carbon in that region is heated sufficiently to evaporate and deposit onto the sample.

2.3 Thin film carbon nanofuse fabrication

The fabrication process is outlined in figure 2. The nanofuses were fabricated on a silicon substrate with a 250 nm thick thermal oxide to provide electrical isolation. Gold pads were made by first spinning 950k PMMA 6 wt% in anisole (MicroChem) on the substrate at 3000 rpm and then placed on a hot plate at 220 °C for 90 s. The PMMA was then exposed with a line dose of 120 $\mu C/cm^2$ using 30 keV electrons from an FEI XL30 ESEM equipped with a high speed beam blanker. The samples were developed using a MIBK:IPA 1:3 mixture (MicroChem) for 60 s, and then spray rinsed with acetone for 2 s followed by a 10 s IPA rinse. A nominal 80 nm gold layer was thermally deposited at $5*10^{-6}$ torr with an evaporation rate of 0.5 Å/s, using 6 nm of chrome as the adhesion layer. The remaining PMMA and gold were then removed with a liftoff process in an acetone bath for 30 min.

A 'bow tie' geometry of the fuse with a narrow neck was chosen because it focuses the current to a small region, allowing the temperature increase to be localized at the middle of the fuse. Patterning the carbon fuses consisted of spinning a positive electron beam resist, 950k PMMA (MicroChem) diluted to 3 wt% in anisole which was spun on at 3000 rpm. The sample was then heat treated on a hot plate at 185 °C for 60 s. The bow tie geometry was exposed into the electron beam resist by exposing the patterned area with a line dose of 230-250 $\mu C/cm^2$ using 30 keV electrons. The sample was developed in a MIBK:IPA 1:3 (MicroChem) solution for 60 s and then spray rinsed with IPA for 10s. A 20 nm thin film carbon layer was next deposited using carbon arc-evaporation at $5*10^{-6}$ torr with an evaporation rate of 3 Å/s. The sample was placed in an acetone bath for 30 min to lift-off the excess carbon, and rinsed with IPA for 10 s. This resulted in a bow tie patterned carbon nanofuse that is electrically connected between two gold contact pads. The samples were then annealed in a 1 inch quartz tube heated to 400 °C for 10

minutes in an argon environment to lower the resistivity of the carbon by approximately 2 orders of magnitude.

Chapter 3 Results and Discussion

3.1 Thin film carbon characterization

To characterize the thin film carbon; its surface roughness, sheet resistance, micro structure, and the carbon sp^2/sp^3 ratio were measured.

The roughness measurement was performed on a 10 nm layer of carbon (as measured by a calibrated x-tal monitor) deposited on an oxidized, polished silicon wafer. The step height and roughness of the carbon film were measured using tapping mode on a Dimension 3100 AFM. Figure 5A and 5B show an AFM step height of 10 nm matched the target thickness, and that the measured roughness of the thin carbon film was 0.53 nm.

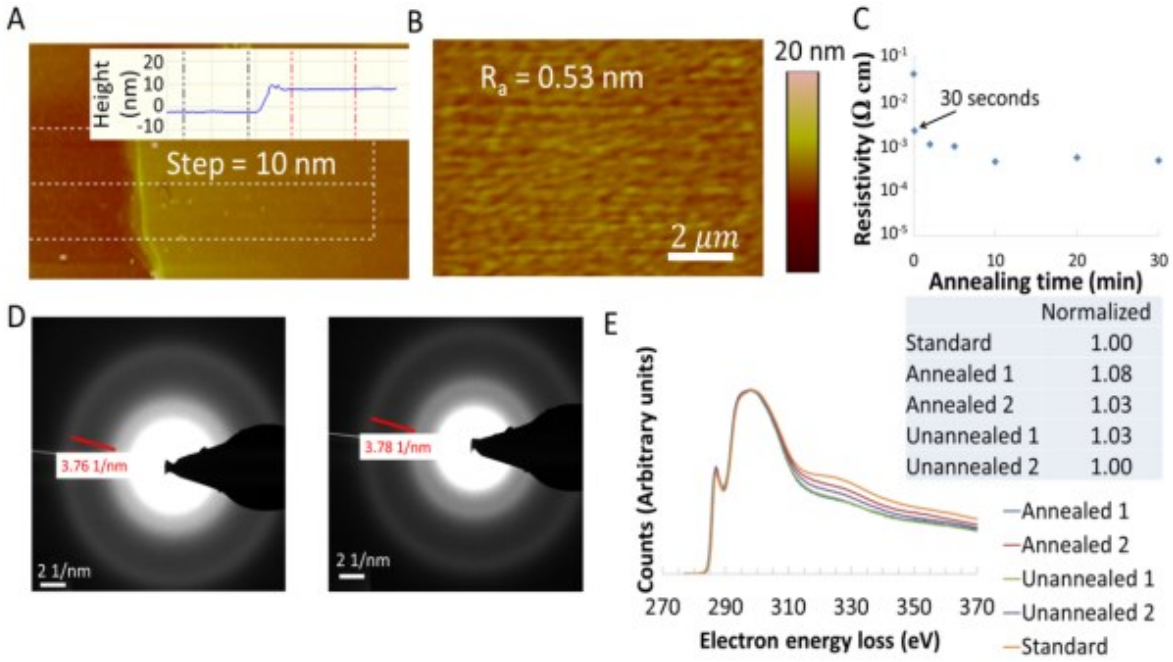

Figure 5 Step height, roughness, and sheet resistance measurements of arc-evaporation thin film carbon. A) AFM measurement showing a 10 nm step height to calibrate the film thickness. The inset is an average over the the dotted box. B) AFM image of the surface and arithmatic average roughness of a thin carbon layer. C) Semi-log plot of the effect of annealing on the sheet resistance of the thin film carbon. D) The diffraction pattern before (left) and after (right) annealing. E) EELS data for annealed and unannealed thin film carbon compared to a sp^2 standard.

The sheet resistivity measurement was performed on a 20 nm thick carbon film deposited on 250 nm thick thermal oxide on a silicon wafer fragment. 4-point probe measurements yielded

an as-deposited resistivity of 0.041 ± 0.007 Ω cm. Previous studies on arc-evaporation carbon have shown that resistivity is reduced by thermal annealing[19]. The impact of annealing in an inert environment at 400 °C was explored. Specifically, the carbon films were annealed in an argon environment for various times. The effect of annealing time on resistivity is shown in figure 5C. Annealing the as-deposited carbon layer at 400 °C for 10 minutes in argon reduced the resistivity by approximately two orders of magnitude.

To determine carbon microstructure and bonding, a 10 nm layer of carbon was deposited onto a flat salt crystal. The carbon film was released from the salt crystal by placing it briefly in a water bath and then rinsed for one hour in another water bath. The carbon film was divided into two samples and placed onto a 300 mesh titanium TEM grid and dried in air. One of the carbon samples was annealed for 10 minutes in an argon environment. To characterize the microstructure, composition, and chemical bonding of the carbon, a Technai F20 TEM was used to obtain diffraction patterns, energy dispersive x-ray spectroscopy (EDX) data, and electron energy loss spectroscopy (EELS) data. The diffraction pattern showed that the thin film carbon is amorphous (figure 5D). In analyzing the EELS results (figure 5E), a strong sp^2 peak is visible. We compared the arc-evaporated thin film of carbon with sp^2 standards (lacey carbon film and ultra-thin carbon black, Ted Pella product # 01824).

3.2 Nanofuse characterization

Figure 6 shows SEM images of 4 carbon nanofuses with varying neck widths, and also I-V plots with varying neck widths for 73 carbon nanofuses. In the SEM images, the dark bow tie shaped region is the carbon fuse. The widths of the middle regions of the fuses varied from 200 nm to 60 nm. Above and below the fuse, the electrically insulating SiO_2 layer (the lighter region)

is visible. Bumps like those on the carbon in figure 6A were seen on a few devices, which we attribute to residue from the lift off process. Current-voltage (I-V) measurements were used to determine the voltage and current required to write to a fuse. For this measurement, a voltage starting at 0 V and increasing at a rate of 0.5 V/s was applied to an intact fuse until the current abruptly dropped to zero, indicating that the fuse has oxidized and is blown. The voltage at

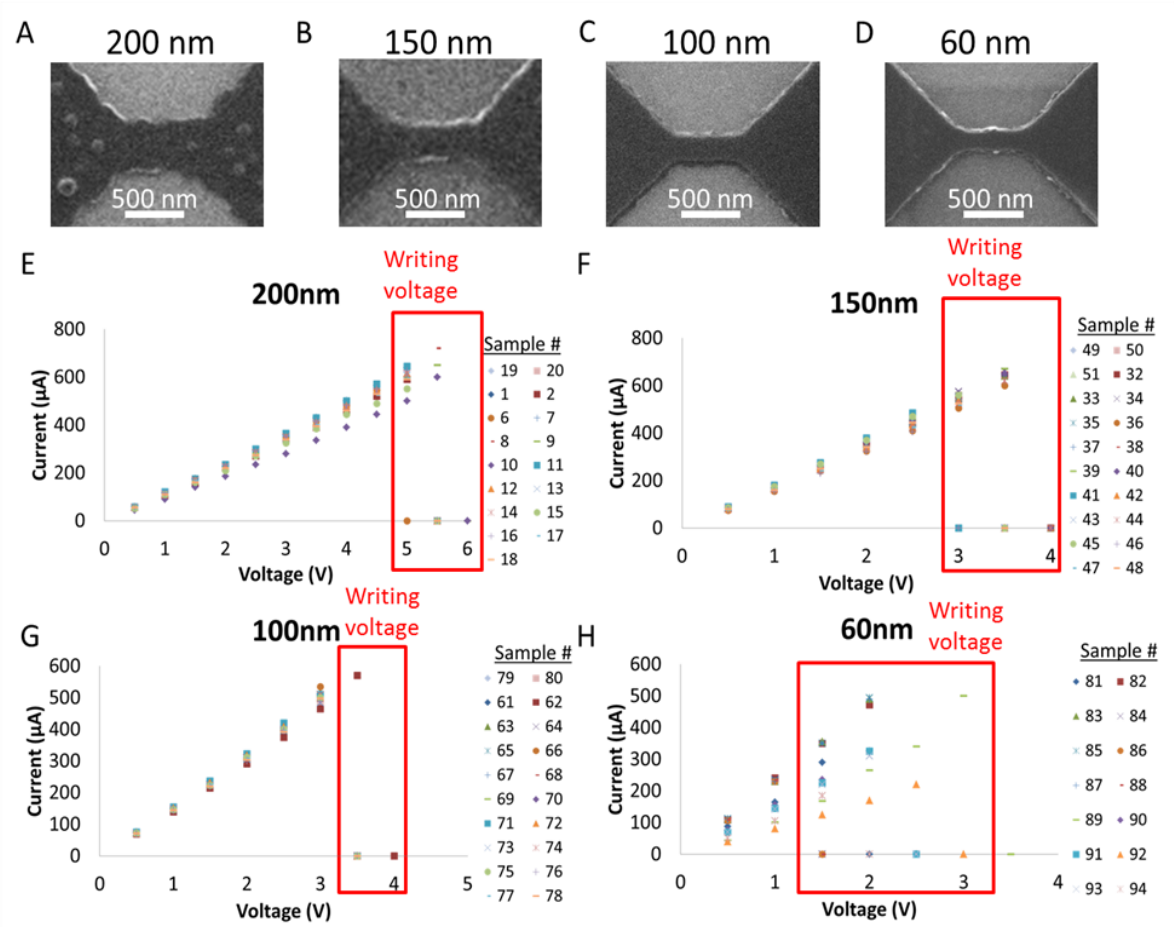

Figure 6 I-V plots for 73 different thin film carbon nanofuses of 4 seperate widths. A-D) SEM micrographs of the nanofuses (from left to right) of 17 fuses with a 200nm width, 20 fuses with a 150nm width, 20 fuses with a 100nm width, and 14 fuses with a 60nm width. The scale bars are all 500nm A) The little spheres on the nanofuse is residual electron beam resist. It did not affect the testing of the nanofuses. Nanofuses were subjected to increasing voltage until they blew. E-H) I-V curves of the the corresponding thin film carbon nanofuses. The red boxes capture the voltage ranges over which the fuses blow. A voltage below this range did not blow any fuses, while a voltage above this range was sufficient to blow all fuses of the noted width.

which the current dropped to zero is the writing voltage, and the slope of the I-V curve shows the resistance of the fuses. For the 200 nm, 150 nm, 100 nm, and 60 nm fuses, the measured writing voltages were 5.1±0.3 V, 3.3±0.3 V, 3.0±0.1 V, and 1.8±0.6 V respectively. These voltages give a range where any voltage below would not change the nanofuse, while any voltage above would result in a blown fuse.

To measure the time required to write to a carbon nanofuse, a square voltage pulse that was 50% higher than the writing voltage was applied using a Hewlett-Packard 214B pulse generator (refer to figure 7F for a schematic of the setup). The voltage across a 1 kΩ resistor in series with the carbon nanofuse was used to measure the current passing through the fuse. When the current dropped toward zero, the fuse was considered to be blown. To ensure the nanofuse was blown, a voltage was later applied across the nanofuse and no current was measured. The current decay seen in figure 7F indicates a write time of less than 200 ns.

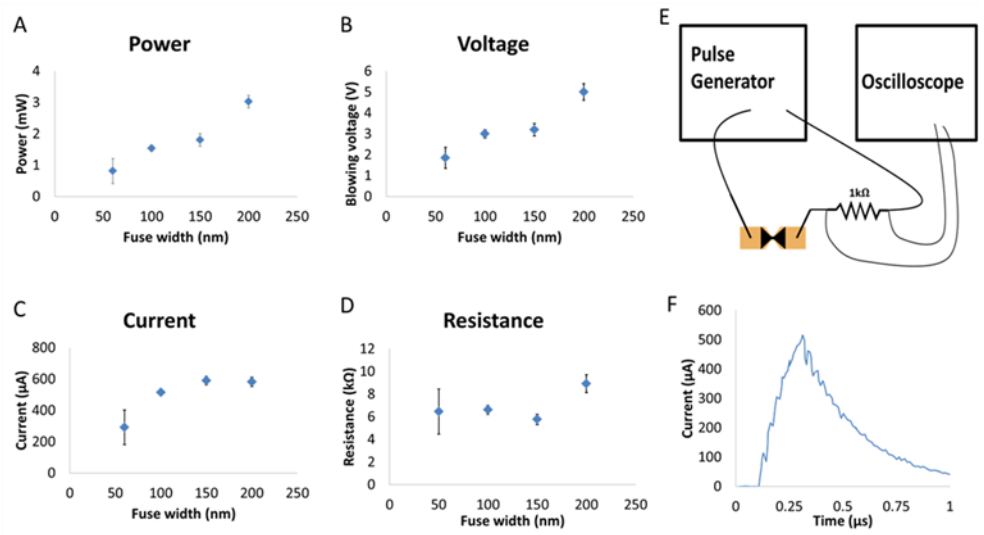

Figure 7 Electrical requirements to write data as a function of fuse width. A) Using the maximum current and voltage the nanofuses could handle before they broke, the power it takes to blow the fuses was found. The resistances of the fuses were obtained by averaging the voltage and current for each fuse. B) Voltage required to blow a nanofuse. C) Current requirements to blow a nanofuse. D) Resistance of the nanofuses. E-F) Schematic of short pulse writing setup with graph of a nanofuse blowing quickly. E) A voltage pulse is applied to the carbon nanofuse, and an oscilliscope measures the voltage over a 1 kΩ resistor to get the current and shape of the pulse. F) Current passing through the 1kΩ resistor during the pulse, resulting in fuse blow within 200ns.

The electrical read stability of carbon nanofuses was tested by applying a constant read voltage of 1 V (well below the writing voltage) over an intact fuse and monitoring the current over time. To accelerate the testing of written carbon and metal fuses, a voltage of 10 V (well above the writing voltage) was applied. Figure 8 shows the electrical read stability of carbon nanofuses and the electrical instability of metal nanofuses due to structural degradation.

3.3 Discussion

Significant variation in the writing voltage is unacceptable for a data storage medium. This voltage variation can come from the film roughness, manufacturing imprecision, and grain boundaries. The low roughness of the carbon film allows the fuses to have a repeatable blowing voltage with a thickness of 20 nm. Since the carbon is amorphous (see figure 5D), there are no grain boundaries that would cause resistivity variations from fuse to fuse. Fuse to fuse resistivity variations would also cause a variation of the blowing voltage.

The high degree of reproducibility of the I-V measurement for 200, 150, and 100 nm indicate that slight process variations do not have a significant impact on device performance (Figure 6). At 60 nm, however, we see greater device-to-device variation in the I-V curves, likely resulting from the larger impact of our lithography limitations and line edge roughness on these smaller devices.

For the nanofuses to be used in data storage, the read and write voltages should work with standard computer drivers. This means that the write voltage should be below 3 V and the read voltage around 1 V. As the nanofuse width gets smaller, the voltage and current required to write them also decreases (figure 7). This trend allows for carbon nanofuses to have the blowing voltage tuned to above 1 V and below 3 V. To analyze any chemical bonding change in the

carbon film from annealing, we compared the normalized intensity ratio of the carbon k edge from the annealed and unannealed samples against sp^2 carbon standards (lacey carbon film and ultra-thin carbon black, Ted Pella product # 01824)[26]. These EELS results indicate that the thin film carbon is composed of amorphous sp^2 carbon both before and after annealing. In short, despite the large change in resistivity due to annealing, no change in the structure, composition, or bonding of the thin film carbon was observed.

The life expectancy of permanent data storage media depends on the failure mechanisms present when data is being read, called read disturb errors, and when it is being stored, called data retention errors. Failure mechanisms in nanofuse based data storage could include atomic diffusion, electro-migration, oxidation, and other chemical changes. The key to having a long timescale for these degradation mechanisms is the fundamental stability of the chemical bonds of the materials that comprise the data storage medium. Sp^2 carbon has a very high local bond strength which should provide a significant stability advantage leading to longer life expectancies. The chemical path most likely to result in degradation of surface carbon is oxidation, but carbon does not readily oxidize below 300 °C, and so would remain very stable at or near room temperature. We have seen no degradation in written or unwritten carbon nanofuses upon storage at room temperature over the several months this work was carried out.

Despite the high expected stability of carbon bonds in the bulk of these materials, we were particularly concerned about the surface carbon atom stability and in particular their stability under the read disturb conditions of data readout. Stability problems for metal fuses have been seen to primarily arise from the formation of dendrites in fuse gaps under applied electric fields (figure 8 E-F), resulting in current pathways when the fuse is broken, and data corruption. We therefore subjected carbon fuses to an accelerated testing of read disturb

conditions and presented the results in figure 8 C-D. For both the intact and blown states of the nanofuse, the test voltage was applied for a time equivalent to the cumulative time that voltage would be applied during 10^{12} reads, without detecting any change in the nanofuses.

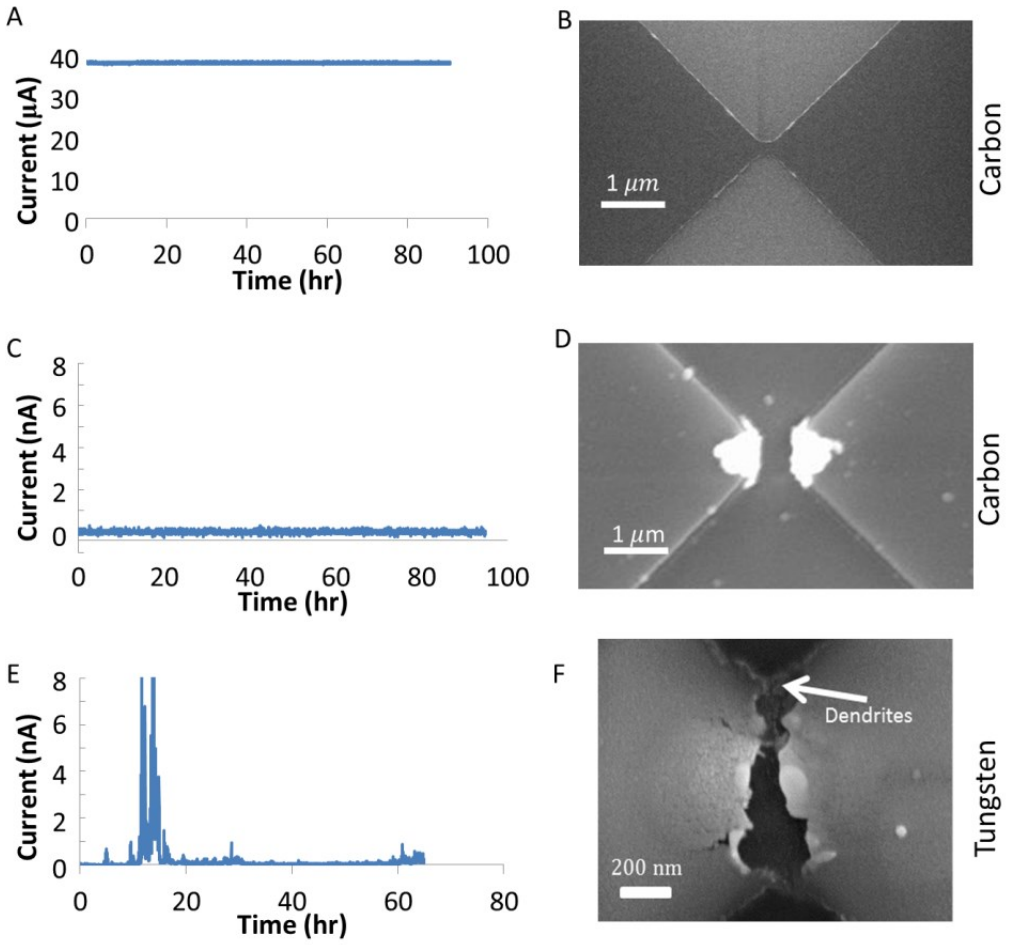

Figure 8 Stability Testing. Programmed "on" (intact) and "off" (blown) state stability in carbon and tungsten fuses under an electrical load. Figures A)-B) are a prorammed "on" state, C)-D) are a programmed "off" state for a carbon fuse, and E)-F) are a programmed "off" state for a tungsten metal fuse. A) "On" state stability for an intact fuse with 1V applied for 90 hours. B) SEM image of intact fuse after bias was held across it. C) "Off" state stability for a blown carbon fuse with a 10V bias held over it for over 90 hours, corresponding to a cumulative time of $\sim 10^{12}$ reads. D) SEM image of a blown fuse after a 10V bias was held across it. E) "Off" state stability for a blown tungsten metal fuse with a 10V bias across it showing unstable current due to dendrite formation. F) SEM image of dedrite growth on the tungsten metal fuse after bias was applied.

Data retention measurements on these fuses during storage are also important but will need to be carried out on far more devices than the few measured here. For such data to be relevant in the context of modern memory systems, this will require scale up (ultimately to GB levels) of integrated devices so that relevant statistical analysis can be done and compared with other archival solid state storage media[27].

Chapter 4 Conclusion and Future Work

4.1 Conclusion

Nanofuses for permanent data storage could be reliably produced with arc-evaporated carbon. The arc-evaporation carbon thin film shows predominantly sp^2 character, is electrically conductive, and deposits uniformly. These carbon nanofuses are electrically stable for read voltages held over 90 hours. Their writing time is under 200 ns, and the carbon nanofuses blow with power in the low milliwatt range. We also studied the voltage and current requirements for fuses in lateral geometries up to 5 times smaller than the previous work on graphene nanofuses. The power and voltage required to blow a carbon nanofuse both decrease with fuse size, indicating that the writing voltage is tunable to fuse geometry. These studies provide data that will be valuable in determining the feasibility of manufacturing permanent memory from arc-evaporated amorphous carbon and in determining productive fuse geometries.

4.2 Future work

Modern storage devices are required to have high data density (>1 Gb/cm^2), read and write data quickly (~Gb/s), and use low power. In addition to these requirements, a permanent data storage device also needs to have high data stability both under normal operating conditions and during storage. In this work we have shown that these carbon nanofuses can use low power during reading/writing. To meet these remaining requirements, the next challenges for these carbon nanofuses to overcome include: 1) Incorporating a passivation layer to enable high density integration, 2) reducing the size of the carbon nanofuses to decrease the power while

reading and writing, 3) design and fabricate a prototype, and 4) reduce the writing time to the nanosecond range to increase the writing speed,

A passivation layer for the carbon nanofuses could allow for multiple layers of carbon nanofuses to be fabricated on top of each other, increasing the data density. In our group, we have briefly investigated a 250 nm layer sputtered of $Si_xO_yN_z$ onto the carbon nanofuses before testing. Even without direct access to air the nanofuses were still capable of blowing. We attribute this to diffusion of oxygen that is trapped inside the $Si_xO_yN_z$ layer. When using the ramping setup to slowly blow the fuses, the passivation layer over the carbon nanofuses remains intact. But when the carbon nanofuses are blown with a pulse the passivation layer has ruptured. This rupturing of the passivation layer during writing could affect adjacent layers of carbon nanofuses, limiting the maximum data density that the carbon nanofuses could achieve, and could alter adjacent bits. Finishing the passivation layer work should be the next priority.

We were able to achieve fuse neck widths down to 60 nm using our current fabrication approach. Decreasing the width of the neck beyond this resulted in the carbon nanofuses breaking without any voltage. It is unclear in our present work whether the 60 nm limit is due to stresses on the carbon thin film exceeding the carbon strength, or the wet lift off step is destructive. We believe that either of these problems could be solved by replacing the wet lift off process with a dry etch that uses a structurally stable hard mask. By first depositing carbon, then using a negative electron resist to make a mechanically rigid nanofuse, we could transfer the nanofuse pattern to the carbon by using an oxygen plasma. Using this process could also allow feature sizes smaller than lithographic features by over etching the material under the mask.

The carbon nanofuses have only been fabricated in isolated devices to test the electrical and physical properties. Next, these carbon nanofuses should be fabricated into a prototype with

many connected nanofuses in crossbar array geometry. Using this device of connected carbon nanofuses we could test the life expectancy, data retention, and read disturb of the carbon nanofuses. This array of carbon nanofuses could also allow for understanding of how blowing a carbon nanofuse could affect the carbon nanofuses around it.

Decreasing the time it takes to write a carbon nanofuse would make these carbon nanofuses more competitive. With the nanofuses in a crossbar geometry, writing to multiple bits at a time becomes possible, further increasing the writing speed. Macroscopic fuses have a relation of $I^2t = c$, where I is the current through the fuse, t is the time it takes to write a fuse, and c is a constant. This relation shows that increasing the current in the fuse a small amount will greatly decrease the time required to write to the fuse. Whether the carbon nanofuses follow this relation as the feature sizes reach the nanoscale remains to be answered.

Bibliography

1. Schwerin, R., Time Capsule. *Oracle magazine* 2014.
2. Lunt, B. M. In *How Long Is Long-Term Data Storage?*, Archiving, 2011.
3. Dobrusina, S. A.; Ganicheva, S. I.; Tikhonova, I. G.; Velikova, T. D.; Zavalishin, P. E., Influence of external factors on the longevity of information recorded on DVD±R discs. *Scientific and Technical Information Processing* **2007,** *34* (5), 258-263.
4. Judge, J. S.; Schmidt, R. G.; Weiss, R. D.; Miller, G. In *Media stability and life expectancies of magnetic tape for use with IBM 3590 and digital linear tape systems*, Mass Storage Systems and Technologies, San Diego, Ca, Technologies, t. I. t. N. G. C. o. M. S. S. a., Ed. IEEE Computer Society: San Diego, Ca, 2003.
5. Oracle. Successful Data Migration *Oracle White Paper* [Online], 2011.
6. Svrcek, I. *Accelerated Life Cycle Comparison of Millenniata Archival DVD*; Life Cycle and Environmental Engineering Branch Naval Air Warfare Center Weapons Division, 2009.
7. Lunt, B. M.; Hansen, D.; Linford, M., Optical Disc Life Expectancy: A Field Report. **2011**, OMD10.
8. Wang, H.; Lunt, B. M.; Gates, R. J.; Asplund, M. C.; Shutthanandan, V.; Davis, R. C.; Linford, M. R., Carbon/ternary alloy/carbon optical stack on mylar as an optical data storage medium to potentially replace magnetic tape. *ACS applied materials & interfaces* **2013,** *5* (17), 8407-8413.
9. Abbott, J.; Niederhauser, T. L.; Hansen, D. P.; Perkins, R. T.; Bell, D. A.; Bard, E. C.; Lunt, B. M.; Worthington, M. O.; Miller, C. M.; Hyatt, D. F., Carbon-coated tellurium for optical data storage. *ACS Applied Materials & Interfaces* **2010,** *2* (8), 2373-2376.
10. Lunt, B. M.; Linford, M. R. In *Towards a True Archival-Quality Optical Disc*, International Symposium on Optical Memory, Nagasaki, Japan, Nagasaki, Japan, 2009.
11. Taur, Y.; Ning, T. H., *Fundamentals of Modern VLSI Devices, 2nd ed.* Cambridge University Press: New York, 1998.
12. Lenzlinger, M.; Snow, E. H., Fowler-Nordheim Tunneling into Thermally Grown SiO2. *Journal of Applied Physics* **1969,** *40* (1), 278-283.
13. Hnatek, E. R., Bipolar Prom Reliability. *Microelectronics and Reliability* **1978,** *18* (4), 325-332.
14. Pearson, A. C.; Jamieson, S.; Linford, M. R.; Lunt, B. M.; Davis, R. C., Oxidation of graphene 'bow tie' nanofuses for permanent, write-once-read-many data storage devices. *Nanotechnology* **2013,** *24* (13), 135202.
15. Novoselov, K. S.; Fal'ko, V. I.; Colombo, L.; Gellert, P. R.; Schwab, M. G.; Kim, K., A roadmap for graphene. *Nature* **2012,** *490* (7419), 192-200.
16. Paton, K. R.; Varrla, E.; Backes, C.; Smith, R. J.; Khan, U.; O'Neill, A.; Boland, C.; Lotya, M.; Istrate, O. M.; King, P., Scalable production of large quantities of defect-free few-layer graphene by shear exfoliation in liquids. *Nature materials* **2014,** *13* (6), 624-630.
17. Ohring, M., *Materials Science of thin Films, 2nd ed.* Academic Press: California, 2002.
18. Blue, M. D.; Danielson, G. C., Electrical Properties of Arc-Evaporated Carbon Films. *Journal of Applied Physics* **1957,** *28* (5), 583-586.

19. Rao, J.; Lawson, K. J.; Nicholls, J. R., The characterisation of e-beam evaporated and magnetron sputtered carbon films fabricated for atomic oxygen sensors. *Surface and Coatings Technology* **2005,** *197* (2-3), 154-160.
20. Ager, J. W.; Anders, S.; Anders, A.; Brown, I. G., Effect of intrinsic growth stress on the Raman spectra of vacuum-arc-deposited amorphous carbon films. *Applied Physics Letters* **1995,** *66* (25), 3444-3446.
21. Dimitriadis, C. A.; Hastas, N. A.; Vouroutzis, N.; Logothetidis, S.; Panayiotatos, Y., Microstructure and its effect on the conductivity of magnetron sputtered carbon thin films. *Journal of Applied Physics* **2001,** *89* (12), 7954-7959.
22. Besold, J.; Thielsch, R.; Matz, N.; Frenzel, C.; Born, R.; Mobius, A., Surface and bulk properties of electron beam evaporated carbon films. *Thin Solid Films* **1997,** *293* (1-2), 96-102.
23. Rebollo-Plata, B.; Lozada-Morales, R.; Palomino-Merino, R.; Portillo-Moreno, O.; Jiménez-Sandoval, S.; Zelaya-Angel, O., High conductivity a-C:N thin films prepared by electron gun evaporation. *Materials Characterization* **2007,** *58* (8-9), 809-816.
24. Pearson, A. C.; Singh, B.; Linford, M. R.; Lunt, B.; Davis, R., Materials Study of Nanoscale Fuses for Solid State Data Storage. In *International Symposium on Optical Memory*, Tokyo, Japan, 2012.
25. Laughlin, K. R.; Jamieson, S.; Pearson, A. C.; Wang, H.; Vanfleet, R. R.; Davis, R. C.; Linford, M. R.; Lunt, B. M., Thin-Film Carbon Nanofuses for Permanent Data Storage. *Acs Omega* **2017,** *2* (6), 2432-2438.
26. Brydson, R.; Zhili, Z.; Brown, A., Revisiting the determination of carbon sp2/sp3 ratios via analysis of the EELS carbon K-edge. **2008**, 357-358.
27. Yamazaki, S.; Iwasaki, T. O.; Hachiya, S.; Takahashi, T.; Takeuchi, K., A 72% error reduction scheme based on temperature acceleration for long-term data storage applications: Cold flash and millennium memories. *Solid-State Electronics* **2016,** *121*, 25-33.

Appendix: Locations and SOPs

Here are the locations and standard operating procedures (SOP) for all of the equipment used in this research.

Chrome and Gold Deposition

To deposit chrome and gold, the thermal evaporator "JIM" found in U238 in the Eyring Science Center is used.

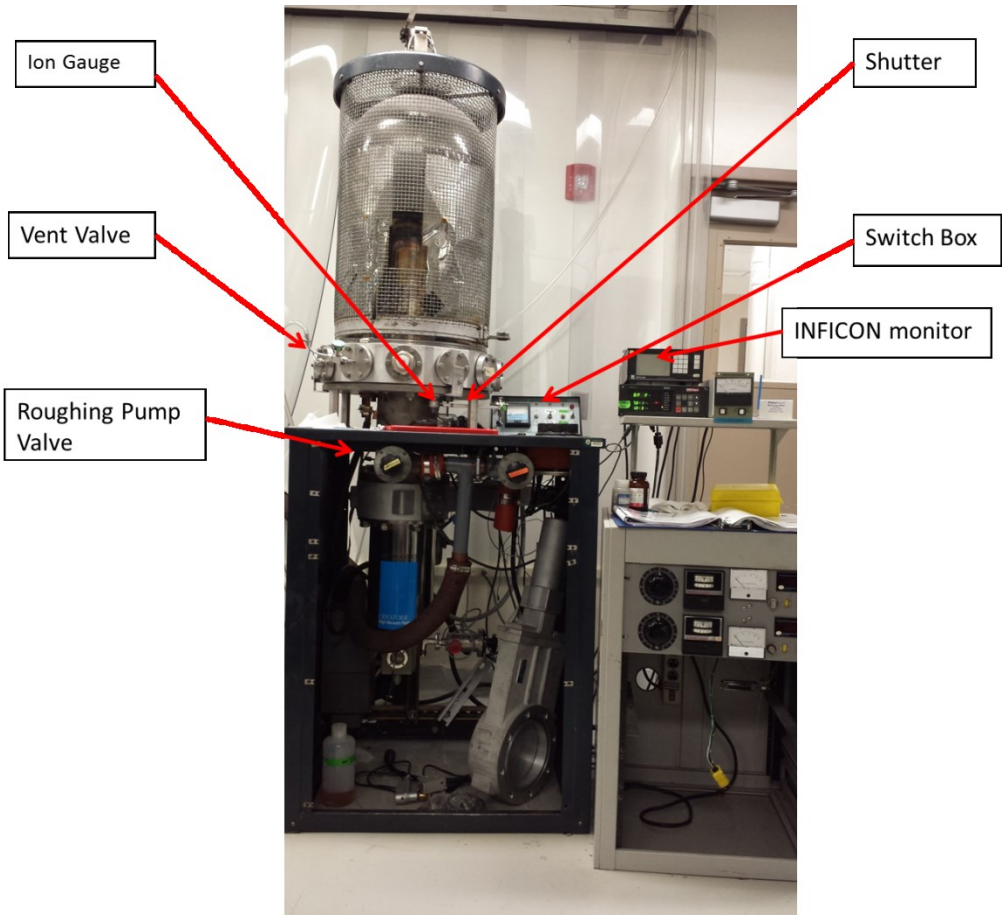

1. Vent the chamber

1.1. Double check to make sure that the chamber is ready to be vented.

1.1.1. The ION GAUGE should be OFF (the bulb is NOT lit). If the bulb is ON, turn it off with the EMIS button.

1.1.2. Make sure the GATE VALVE is CLOSED.

1.2. Open the Nitrogen tank in the corner; record the pressure on the log sheet. Then open the back little black valve on the regulator.

1.2.1. Make sure the left gauge is around 20 psi. The metal valve opens when rotated clockwise.

1.2.2. Make sure that you close the nitrogen tank when you are done.

1.3. Open the VENT VALVE.

1.4. Wait until the chamber pressure (TC1) reads 7.6 +2 (760 torr, this is atmospheric pressure)

1.5. Raise the bell jar a little bit using the RAISE button, and then turn of the VENT VALVE.

1.6. Raise the jar the rest of the way.

2. Prepare your sample

2.1. Look for a location on the plate where your sample will be shielded from the Gold AND Chrome when the SHUTTER is closed, and exposed to the Gold AND Chrome when SHUTTER is open.

2.2. Tape your sample to that location using the VACUUM TAPE

2.3. Obtain both the GOLD BOAT and CHROME ROD located in the top drawer of a black shelf box.

2.4. Place the boats in their respective holders.

2.5. If needed, replace the GLASS SLIDE WINDOW.

3. Check the CRYSTAL MONITOR (XTAL)

3.1. Turn on the INFICON monitor if it is not already on.

3.2. Push the XTAL button (button number 1), if the XTAL reading is 100%, change the CRYSTAL.

4. Pump down the CHAMBER

4.1. Lower the bell jar slowing using the LOWER button, make sure that the coating of the jar does not get caught on the sample holder. Make sure it makes a good seal.

4.2. Make sure the VENT VALVE is CLOSED.

4.3. SLOWLY open the ROUGHING PUMP VALVE, and start a timer for T_{ROUGH} in the JIM logbook.

4.3.1. Keep the foreline pressure (TC2) BELOW 3.0 +2.

4.4. When the pressure reads 1.5 +0 (1.5 torr) CLOSE the ROUGHING PUMP VALVE and record T_{ROUGH}.

4.5. Open the GATE VALVE, and start T_{CRYO}.

4.6. Wait for ~30 seconds and turn on the ION GAUGE by pressing the EMIS button.

4.6.1. The filament should turn on, looking like a light bulb.

4.7. When the pressure reaches 5.0 -5 ($5 * 10^{-5}$ torr) record T_{CRYO}.

4.8. Wait until the chamber reaches 5.0 -6 ($5*10^{-6}$ torr), this usually takes around 20 minutes or so.

5. Deposition of Chrome

5.1. Make sure that the INFICON monitor is on.

5.2. Change the settings of DENISTY, Z-RATIO, and TOOLING FACTOR.

5.2.1. Press the PROG button.

5.2.2. Use the button that has a C with a triangle around it to go up in the menu, and the E with a triangle around it to go down until you are over the desired parameter.

5.2.3. To change the parameter, just type in the numbers. When the numbers are what they should be, hit the E triangle button.

Material	Density	Z-Ratio	Tooling
Chrome	7.200	0.305	63.0
Gold	19.30	.381	63.0

5.3. Flip the BOAT SELECTION toggle switch to the REAR BOAT.

5.4. Flip the FILAMENT toggle switch to on. This turns on the power supply.

5.5. Ramp up the voltage with a maximum rate of 20 V/Min (5 V/15 Sec) using the VARIAC.

5.5.1. You should not exceed 10 Amps.

5.5.2. Go until you have a deposition rate of around 1Å/s. This can be seen on the INFICON monitor.

5.5.3. The voltage will usually be around 45 V.

5.6. OPEN the SHUTTER, and ZERO the crystal monitor (hit the 3 button that has the word ZERO over it).

5.7. Record everything in the logbook that it asks.

5.8. Wait until the INFICON monitor reads the desired thickness, usually around 0.070 kÅ (this is going to be 7 nm), then CLOSE the SHUTTER.

5.9. Ramp down the voltage at a rate LESS than 20 V/min.

5.10. Turn off the FILAMENT toggle switch.

6. Deposition of Gold

6.1. Flip the BOAT SELECTION toggle switch to the FRONT BOAT.

6.2. Flip the FILAMENT toggle switch to on.

6.3. Ramp up the voltage with a maximum rate of 20 V/Min (5 V/15 Sec) using the VARIAC.
  6.3.1. You should not exceed 10 Amps.
  6.3.2. Go until you have a deposition rate of around 1Å/s.
  6.3.3. The voltage will usually be around 150 V.
6.4. OPEN the SHUTTER, and ZERO the crystal monitor.
6.5. Record everything in the logbook
6.6. Wait until the INFICON monitor reads the desired thickness, usually around 0.750 kÅ (this is going to be 75 nm), then CLOSE the SHUTTER.
6.7. Ramp down the voltage at a rate LESS than 20 V/min.
6.8. Turn off the FILAMENT toggle switch.

7. Vent the chamber and remove sample
7.1. Get the chamber ready to be vented.
  7.1.1. Turn OFF the ION GAUGE by hitting the EMIS button.
  7.1.2. CLOSE the GATE VALVE toggle switch!
7.2. Open the Nitrogen Tank.
7.3. Open the VENT VALVE.
7.4. Wait until the chamber pressure reads 7.6 +2 (760 torr, this is atmospheric pressure)
7.5. Raise the bell jar a little bit using the RAISE button, and then turn of the VENT VALVE.
7.6. Raise the jar the rest of the way.

8. Get the system into standby
8.1. Lower the bell jar slowing using the LOWER button, make sure that the coating of the jar does not get caught on the sample holder. Make sure it makes a good seal.
8.2. Make sure the VENT VALVE is CLOSED.
8.3. SLOWLY open the ROUGHING PUMP VALVE
  8.3.1. Keep the foreline pressure BELOW 3.0 +2.
8.4. When the pressure reads 5.0 -1 (0.5 torr) CLOSE the ROUGHING PUMP VALVE.
8.5. The system is now in standby.

9. REMEMBER TO MAKE SURE THE NITROGEN TANK IS TRUNED OFF!! This includes the main valve on the far right, and the little black valve on the far left.

Carbon Deposition

To deposit carbon, the "Denton" evaporator found in U236 in the Eyring Science Center is used.

NOTE: For the switches, pushing them will turn them on if they are off, and off if they are on.

So to turn on you push the button, to turn it off you push it again.

1. Turn on the system by pressing the black ON SYSTEM switch on the lower left corner of the control panel.
2. Turn on the MECH PUMP switch.
3. Turn the PRESSURE GAUGE SELECTOR to foreline.
4. When the foreline pressure drops below 50 mTorr, open the BACKING VALVE. When the pressure drops below 50 mTorr again, turn on the HI-VAC PUMP POWER SWITCH (NOT the valve!!).
5. Wait for 20 minutes before you go past step 14.
6. Make sure that the ROUGHING VALVE is closed. Vent the chamber by turning on the N2 tank in by the wall, then open the VENT VALVE.
7. When the pressure seal breaks, turn off the VENT VALVE, then the N2.
8. Raise the bell jar to its highest point (you have to lift it yourself, no motors) and then rotate it to the right until it is over the crystal monitor. Lower the bell jar until it supports itself.

9. Sharpen the carbon rods that you will use, and place them in the holder so that there is force between the two pieces of carbon.
10. Replace the boat in the DENTON with the carbon rod holder.
11. Place your sample on the sample holder, and position it so that the carbon will have a straight shot at the surface. (Don't worry about the shutter, we won't be using it)
12. Close the bell jar.
13. Add LN2 (liquid nitrogen) to the funnel until condensation starts to drip off of the outside of the funnel.
14. Do not continue until 20 minutes has passed since step 4.
15. Close the BACKING VALVE.
16. Open the ROUGHING VALVE and start T_{ROUGH}. Turn Pressure selector gauge to foreline.
17. When the pressure drops below 100 mTorr stop T_{ROUGH} and record it in the logbook.
18. Close ROUGHING VALVE and then open the BACKING VALVE.
19. Open the HI-VAC VALVE, start T_{CRYO}.
20. Turn on the high vacuum gauge, record T_{CRYO} when the pressure reaches $1*10^{-5}$ Torr.
21. Wait until chamber drops below $5*10^{-6}$ Torr. This can take around 30 minutes. Add LN2 if it takes longer. You can do the next step while you wait.
22. Turn on the Crystal monitor, and set these parameters, and check the XTAL crystal and record these in the logbook. Zero the crystal by hitting the 3 button.

Material	Z-Ratio	Density	Tooling
Carbon	3.26	2.25	72

23. Turn on the Fil/Glow Power switch, and ramp up the voltage with a rate of 10%/30seconds.
    23.1. Current should never exceed 200 A, and voltage should remain below 80%.
24. The carbon will start to glow, and get brighter as it evaporates. When it stops glowing, it is done and needs to be sharpened.
25. Lower the voltage at a rate of 20%/30seconds, then turn off the Fil/Glow Power switch when the voltage reaches 0%.
26. Turn off the High Vacuum GAUGE (not the PUMP)
27. Close High Vacuum Valve.
28. Open the N2 tank and then the VENT VALVE.
29. Repeat steps 6-8 to open the bell jar.
30. This process will need to be done a few times in order to get enough carbon coated. If doing more coating, go back to step 9.
31. If you are done for the day.
    31.1. Lower the bell jar
    31.2. Close the Backing Valve

31.3. Open the Roughing Valve
31.4. Bring down the system to 20 mTorr
31.5. Close all of the valves
31.6. Turn off the roughing pump and the high vacuum pump
31.7. Turn off the power.

Electron Beam Lithography

To use the electron beam lithography setup, we used the ESEM is in room 101 in the McDonald building at BYU.

1. Log onto the lithography computer using username: davis and password: 90901.

2. On the left-front corner of the microscope table there are two switch boxes, turn both to 'litho' (channel B)

3. Vent the microscope (in the SEM control program)
4. Scratch your sample so you have something to focus on!
5. Insert sample holder with silicon triangles closest to the left side of the microscope chamber. This gives a convenient coordinate system when looking at the computer monitor, the triangles will be at the top, with the faraday cup to the left of them.
6. Flip the stage ground connection up to 'C'
7. Remove aperture and insert beam blanker. Be careful, don't touch anything that goes in

vacuum without gloves on. Don't touch anything non-vacuum with gloves on.

1. Be sure outer ring of the beam blanker aperture is set to 3 so the blanker is not blocking the beam when not blanked.

8. Pump microscope chamber down.
9. Connect cable to beam blanker
10. Turn on Scanservice Corp. box. Make sure the reading on the display is about 132 and that the knob on the left is set to 'on'.

11. Set-up picoammeter

1. Connect BNC cable to microscope door.
2. Turn on the picoammeter
3. Reset to factory defaults (Push 'menu' until the display says 'Defaults'. Turn wheel until the smaller display on the right says 'Factory', push 'menu' again and wait for the screen to return to reading current.)
4. press the down range button until the display reads XXX.XXX nA (for convenience)
5. Turn off zero check by pressing the zero check button.
6. To set the zero correction, press 'shift' then 'zero check'.

12. Make sure that the stage tilt is at zero
13. Move stage to (600, 7000). Now you should be located above the lower triangle. This has small gold particle on it. The upper triangle has some wagon wheel patterns etched into it.

14. Turn on beam at the desired accelerating voltage (30KeV) and spot size.
15. Focus and set your working distance (WD) to 10 mm.
16. Go to 'Magn', select 'Device photo' and set to 'Display' so that the magnification shown is the magnification calibrated for in NPGS.
17. Do a fine focus and stigmation adjustment.
18. Move to the faraday cup and zoom in so that the hole in the middle fills the screen (20000X).
19. Record the beam current on the picoammeter
20. turn knob on scanservice corp box to 'off'
21. record current on the picoammeter (or make sure that the reading is zero)
    1. The absolute value of the difference between the readings is the beam current.
22. Repeat for any other spot size you will be writing with.
23. Turn scanservice corp box knob back to on.
24. Locate the edge of your sample and make sure that the top of your sample is in focus. Keep in mind that any time you are looking at or near your sample you are exposing it. Do not change your stigmation.
25. In the NPGS “Commands” menu hit Direct Stage control, enter, enter. Move to scratches along the edges and focus then hit spacebar. Move to each new focus point using the manual knobs (not the mouse) and focus/spacebar at each point. Hit enter when done. When it accepts the focus values hit ESC to exit the Direct Stage Control command.
26. Note the coordinates of a starting point on your sample so you will have an idea where your patterns will be written.
27. Turn knob on Scanservice corp box to 'external'
28. Move to the starting spot (center) and zoom to what you set in the parameters
29. On the microscope computer, go to 'Scan' and select 'external xy'
30. Set NPGS parameters
    1. Select pattern to write
    2. Enter measured beam current
    3. Enter desired dosages
    4. Make sure the microscope magnification matches the magnification specified in the NPGS run file
31. Process the NPGS run file and write your patterns
32. When you are done writing be sure to clean up and reset all the changes you made. Follow steps 1-13 in reverse (more or less)
    1. return stage to (600,6000) and set your WD to 15-20 mm
    2. turn off the beam on the SEM computer
    3. turn off and disconnect the picoammeter
    4. Turn off the Scanservice corp box and disconnect the cable from the beam blanker. Leave the beam status on “ON.”
    5. Vent the chamber
    6. replace the aperture and put the beam blanker away
    7. Remove sample holder. Put sample holder in its jar and return it to its drawer.
    8. Flip stage ground switch down to 'A'
    9. Pump down chamber
    10. make sure both data switches on the left corner of the table are returned to

'OIM/EDAX' (channel A)

11. Put the computer back to the other by hitting CTRL twice.